

## Supplementary Materials

### Photocatalytic CdSeQDs-decorated ZnO nanotubes: an effective photoelectrode for splitting water<sup>†</sup>

**Neelu Chouhan,<sup>a</sup> Chai Ling Yeh,<sup>b</sup> Shu-Fen Hu,<sup>\*c</sup> Ru-Shi Liu,<sup>\*a</sup>  
Wen-Sheng Chang<sup>d</sup> and Kuei-Hsien Chen<sup>e</sup>**

<sup>a</sup>Department of Chemistry, National Taiwan University, Sec. 4, Roosevelt Road, Taipei 106, Taiwan.

Email: [rsliu@ntu.edu.tw](mailto:rsliu@ntu.edu.tw)

<sup>b</sup>Institute of Electro-Optical Science and Technology, National Taiwan Normal University, 88, Sec. 4, Ting-Chou Road, Taipei 116, Taiwan.

<sup>c</sup>Department of Physics, National Taiwan Normal University, 88, Sec. 4, Ting-Chou Road, Taipei 116, Taiwan. Email: [sfhu.hu@gmail.com](mailto:sfhu.hu@gmail.com)

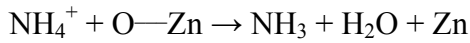
<sup>d</sup>Department of Nano-Tech Energy, Industrial Technology Research Institute, 421, Sec.4, Zhong Xing Road, Jhun Dong, Hsinchu 310, Taiwan.

<sup>e</sup>Institute of Atomic & Molecular Sciences Academia Sinica, Sec. 4, Roosevelt Road, Taipei 106, Taiwan.

\* To whom correspondence should be addressed. Email: [rsliu@ntu.edu.tw](mailto:rsliu@ntu.edu.tw) and [sfhu.hu@gmail.com](mailto:sfhu.hu@gmail.com)

## ZnO NRs and NTs Synthesis

ZnO seeds were cast on an FTO surface using an alcoholic solution of bidentate-0.002 M zinc acetate and heating for 0.5 h at 350 °C. Aqueous chemical growth (ACG)<sup>16</sup> was used to synthesize the arrays of ZnO NTs or NRs on ZnO-seeded FTO using a growth solution of zinc nitrate hexahydrate ( $\text{Zn}(\text{NO}_3)_2 \cdot 6\text{H}_2\text{O}$ , 3.57 g, 0.06 M; JT Baker) and hexamethylenetetramine (HMT;  $(\text{CH}_2)_6\text{N}_4$ , 1.68 g, 0.06 M; ACROS Chemicals) in 200 mL deionized water (DIW) in a 250 mL glass beaker. The substrate with the ZnO seed was horizontally suspended in this growth solution. After the beaker had been covered with Al-foil, was kept in a furnace at 88-92 °C for 48 h at ambient pressure without addition of any catalyst. Thereafter, the grown material was cooled slowly for 0 h, 12 h, 24 h and 36 h and then annealed at 450 °C for 30 min. The uncooled ZnO samples grew as rods and the array films in the mother solution were slowly cooled for different times to promote the hexagonal etching of NRs, facilitating their gradual conversion into NTs (Fig. 1). Since  $\text{NH}_3$  gas that was liberated during the cleavage of HMT was collected over the solution, it began to dissolve upon cooling to produce  $\text{NH}_4\text{OH}$ . The concentration of  $\text{NH}_4\text{OH}$  rose with the both an increase in time and a decline in temperature, resulting in the gradual transformation of the nanostructure from rods to tubes. Because under thermodynamic equilibrium conditions, the facets (0002) of high surface energy grow with small area, while the lower energy facets ( $(01\bar{1}0, 2\bar{1}\bar{1}0)$ ) are larger (X.Y. Kong and Z. L.Wang, *IEEE* 2004, 894). High surface energy leads instability to the nanorods, which gradually tends to etch nanorod with  $\text{NH}_3$  by slow cooling and in aqueous medium it gives  $\text{NH}_4^+$  and  $\text{OH}^-$  ions. XAS study reveals that the top of the ZnO NRs are oxygen rich and when this oxygen rich-end attacked by  $\text{NH}_4^+$ , it causes etching. Following is the plausible chemical pathway to etch the nanorod surface that may lead to form ZnO nanotube.



Etching begins from the centre of basal surface of ZnO, which is the highest surface energy point. Hence, centre of basal surface is more vulnerable to be attacked by etching species.

A comparative study of uncooled (ZnO NRs) and 24 h- cooled (ZnO NTs) samples of tabular ZnO was carried out. The ZnO NTs/NRs arrays films were washed with DIW, air-dried and annealed at 450 °C for 0.5 h.

### CdSe-QDs Production

CdSe QDs were synthesized using the method described by Qu and Peng *et al.*<sup>17</sup> with some modifications. As-synthesized oleic acid escorted-hydrophobic-CdSe QDs (UV-visible spectrum of oleic acid escorted-CdSe QDs, synthesized at different time intervals were shown in Fig. S†1) were not found suitable to be attached to ZnO nanostructures. Hence, these CdSe QDs adopted hydrophilic character upon the exchange of ligands (oleic acid with 3-mercaptopropionic acid (MPA)). Finally, the aggregates of MPA-escorted CdSe QDs were deposited on the surface of the ZnO NTs/NRs arrays by sequential layer-by-layer deposition (ZnO casted-FTO substrate dipped into different concentration i.e. 7, 14, 28, 56, 63 nM of MPA-escorted CdSe QDs solution in methanol, followed by drying in N<sub>2</sub> and the process repeated 30 times) and the as-obtained ZnO NRs or NTs@CdSe(QDs) samples were annealed at 350 °C for 0.5 h. Diffuse reflectance UV-visible absorption spectrum was recorded for solid films of ZnO NRs or NTs@CdSe(QDs) arrays casted on FTO substrate that confirmed the aforementioned deposition, (Figs. S2† a and S2† b). Representative peaks of ZnO nanocrystals were found around 370 nm; those of CdSe QDs belongs to the ZnO NRs@CdSe(QDs) and ZnO NTs@CdSe(QDs) were found at 551 nm and 557 nm, respectively. The 3 nm size of the CdSe particles is calculated from the first excitonic

absorption peak of the UV-Vis spectrum<sup>18</sup> (Fig. S1†), agreed closely with the high-resolution transmission electron microscopic (HRTEM, JEM-2100F microscope) results (Fig. 2d). In Figs. 2a and 2b, the typical fringes associated with 0.26 nm lattice spacing are attributed to the (002) reflection plane of the ZnO NT and loading of the CdSe nano aggregates on the hexagonal edge of ZnO (Fig. 2b). MPA act as linker unit between CdSe QDs and ZnO NRs/NTs species (CdSe(QDs)-HS-(CH<sub>2</sub>)<sub>2</sub>COOH-OZn) (Ratanatawanate *et al.*, *ASC Nano* 2, 2008, 1682 and Sun *et al.*, *Langmuir* 13, 1997, 5168). Here, MPA-anchored to the ZnO nanotube surface (oxygen is typically thought of as a donor atom in ZnO nanotube) through it's the carboxyl groups via the C=O bond of MPA contains empty  $\pi^*$  orbitals and should therefore be a good  $\pi$  acceptor and leaves thiol groups to bind with Cd<sup>2+</sup> via S (Meulenberg *et al.*, *J. Am. Chem. Soc.*, 131, 2009, 6888). Therefore, the nature of bond mention between CdSe- MPA - ZnO is purely chemical. The SAED pattern in Fig. 2c is characteristic of the elongated-hexagonal phase of single crystalline ZnO (JCPDS file no. 077-2205). Figure 2d displays the dispersion of a 3 nm-single CdSe QDs on a ZnO NT and the associated lattice fringes of size 0.162 nm correspond to the 101 plane of CdSe QDs (JPCDS: 077-2307). Figures 2e and 2f present low-magnification field emission scanning electron microscopic (FESEM, JEOL JSM-6700F) images of arrays of pristine ZnO NTs grown in the regular hexagonal fashion. The mean diameter of the ZnO NTs in the array is in the range 250-350 nm; their wall thickness is 40-50 nm; their top area is 0.026  $\mu\text{m}^2$  and their average surface density is ca. 5 rods per  $\mu\text{m}^2$ . Figure 2f shows a cross-sectional view of the ZnO NTs, which reveals that the vertically well aligned ZnO NTs have a length of around 5  $\mu\text{m}$ . The crystallinity and crystalline structure of the CdSe(QDs)-decorated ZnO NTs were investigated using X-ray diffraction (XRD, X'Pert PRO advanced automatic diffractometer with Cu  $K_\alpha$  radiation, operated at 45 kV and 40 mA and  $\lambda = 1.5406 \text{ \AA}$ ). Figures S3†c, S3†d, S4†e and S†4 (black, red and green) present the XRD patterns of pristine ZnO NTs (24 h

cooled), ZnO NTs@CdSe(QDs) and annealed ZnO NTs@CdSe(QDs). They demonstrate that highly oriented single crystalline ZnO NTs grew along the 002 plane on FTO, consistent with JCPDS file no. 077-2205 (Figs. S3†b). The low surface energy of the 100 and 101 planes than of the preferred plane 002 favored the alignment of ZnO NTs along the c-axis, promoting the growth of ZnO layers along the c-axis.<sup>19</sup> Characteristic CdSe peaks are not clearly visualized in Figs. S3† d and S3† e because very few QDs were loaded on the ZnO surface but upon careful examination of the enlarged XRD profile of annealed samples, a prominent peak of CdSe at approximately  $2\theta = 42^\circ$  are observed (Fig. S†4). The crystal structures of the CdSe quantum dots are sensitive to synthesis temperature. Zinc-blende XRD patterns of the CdSe nanocrystals were obtained at a synthesis temperature of  $<230^\circ\text{C}$  but wurtzite nanocrystals of CdSe were formed at higher temperatures (above  $270^\circ\text{C}$ ). Herein, CdSe QDs were synthesized at  $280^\circ\text{C}$ , so, as expected, QDs grew in the wurtzite phase. The strong and distinguished peak (110) of CdSe QDs ( $2\theta = 41.99^\circ$ , JCPDS file no. 077-2307) (green line in Figs. S†4 and S3 †a) is associated with the annealed samples was identified by comparison with that of the non-annealed ZnO NTs@CdSe(QDs) samples (Fig. S†4 red lined), which yielded a very weak peak, owing to the encapsulation of CdSe by amorphous MPA, which is autoignited upon annealing at  $350^\circ\text{C}$ . Morphological changes of annealing are visualized in Fig.S†5. Photoluminescence emission spectrum of 3.06 nm oleic acid escorted- CdSe QDs solutions with yellow light emission, excited by a 354 nm light source and micrographic TEM image of oleic acid escorted- CdSe QDs has been showcased in inset are shown in Fig. S†6.

Figure S†7 shows that uncooled ZnO was present as regular hexagonal rods with edge lengths of 100-150 nm, a cross sectional area of  $2.6 \mu\text{m}^2$  with an average rod density of ca. 3.5 rods per  $\mu\text{m}^2$ , a diameter of 200 – 300 nm, and lengths of almost the height of the sample that was cooled for  $\sim 24$  h ( $\sim 4 \mu\text{m}$ ).

### Particle Size and Molecular weight measurement for CdSe QDs

CdSe quantum dots particle size determined (Yu *et al.*, *Chem. Mater.* 15, 2003, 2857) using following equation;

$$D = (1.6122 \times 10^{-9})\lambda^4 - (2.6575 \times 10^{-6})\lambda^3 + (1.6242 \times 10^{-3})\lambda^2 - (0.4277)\lambda + 41.57 \quad (1)$$

In above equation,  $D$  (nm) denotes the size of a nanostructured sample, and  $\lambda$  (nm) is the wavelength of the first excitonic absorption peak (551 nm and 557 nm) of the samples. As a first approximation, the molecular weight of the CdSe nanocrystal can be directly calculated from the hard-core diameter  $\sigma$  and the density of the bulk CdSe semiconductor ( $\delta = 5.816 \text{ gcm}^{-3}$ ). High-resolution TEM images indicate (Fig.2d) that nanocrystals have the same particle size ( $\sigma = 3.06$  and 3.11 nm) as calculated by the help of Eq. 1 and UV visible spectrum , used to measure the molecular weight of the same structures of CdSe nanodots and bulk material. (K. J. Bowen-Katari, V. L. Colvin and A. P. Alivisatos, *J. Phys. Chem.* 98, 1994, 4109 and J. J. Shiang, V. Kadavanich. R. K. Grubbs and A. P. Alivisatos, *J. Phys. Chem.* 99, 1995, 17417) Molecular weight (524,000 and 551,440 g/mol) of CdSe nanocrystals was calculated using Eq. 2,

$$M_n = \frac{\pi}{6} N_A \delta \sigma^3 \quad \dots \dots \quad (2)$$

Where,  $N_A$  is the Avogadro number. Following equation 3 used to yield the mass (mg) of the solid CdSe QDs that is required to prepare a given volume (mL) of the required concentration (mM).

$$\text{Mass(mg)} = \text{concentration(mM)} \times \text{volume(mL)} \times \text{molecular weight}\left(\frac{\text{g}}{\text{mol}}\right) \quad \dots \dots \quad (3)$$

Controlled deposition of QDs (30 dip of ZnO NTs casted on FTO in methanolic MPA-QDs solution) of concentration around 7 mM, 14 mM, 28 mM and 56 mM on a 1D-ZnO surface was performed. The photo-electrochemical responses were tested and the results obtained were applied to estimate the optimum loading of CdSe QDs that was required to maximize the transfer of electrons from CdSe to ZnO in a photoanode of ZnO NTs@CdSe(QDs) arrays.

### **Measurement of the effectiveness of splitting of water**

A pyrex glass three-electrode PEC cell comprises OR a saturated calomel electrode (SCE) as a reference electrode, a Pt flag as a cathode and ZnO NTs@CdSe(QDs) arrays as a working electrode (photoanode). These components were assembled in a double walled reactor and a round quartz window with a diameter of 5 cm. The photovoltaic water splitting performance of the cell was measured under illumination of a 300W Xe light source (>420 nm, Xe lamp-HX1, Model PE300UV, Perkin Elmer) with an intensity of 100 mW/cm<sup>2</sup> (AM 1.5G), regulated using a power-energy meter (Gentec ( $\varepsilon$ ) Solo2 Model-UP12E105-H5) at a constant temperature of 25 °C in an aqueous hole scavenger-electrolyte solution of 0.35 M Na<sub>2</sub>S and 0.25 M K<sub>2</sub>SO<sub>3</sub> (pH = 13.3). The working electrode with a surface area (001) of ~1cm<sup>2</sup> was connected to the circuit via a copper wire using silver paste, and the area beyond the arrays was covered using epoxy resin and teflon tape. The photocurrent density-voltage (*J-V*) characteristic of the samples was monitored using an electrochemical analyzer (Autolab potentiostat model PGSTAT30) that was equipped with GPES (general purpose electrochemical study) manager software. Photographs of the annealed ZnO NTs@CdSe(QDs), ZnO NTs@CdSe(QDs) and pristine ZnO NTs electrode samples were taken (a) in ordinary light and (b) in UV light, are shown in Fig. S†11. Representative spectral distribution of Xe light source with the filter PE300BF in visible light region (390-770 nm), is shown in Fig.12.

**Fig. S1** UV-visible spectra of as-synthesized CdSe(QDs) with TOPO ligands in original solution at different time intervals.

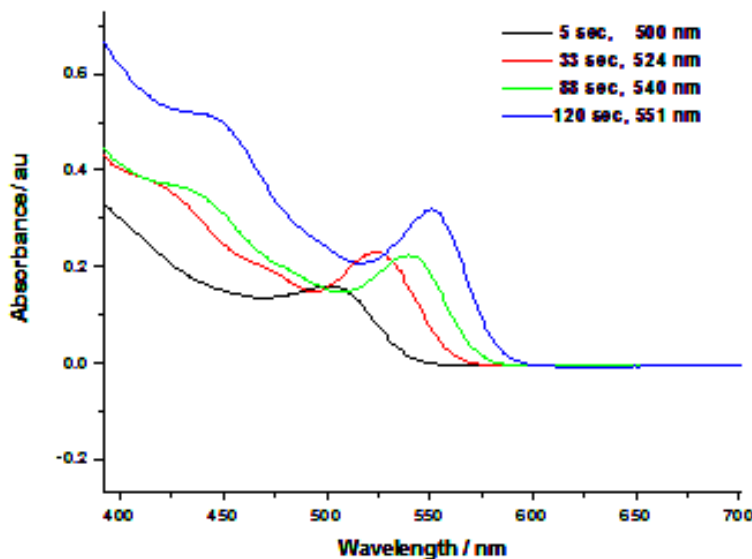


**Fig. S2** UV-visible spectra of (a) pristine ZnO nanorods and nanotube samples and (b) ZnO NRs@CdSe(QDs) and ZnO NTs@CdSe(QDs). Representative Peak of, ZnO around 370 nm and CdSe at 551and 557 nm for ZnO NRs@CdSe(QDs)and ZnO NTs@CdSe(QDs), respectively are appeared in both graphs.

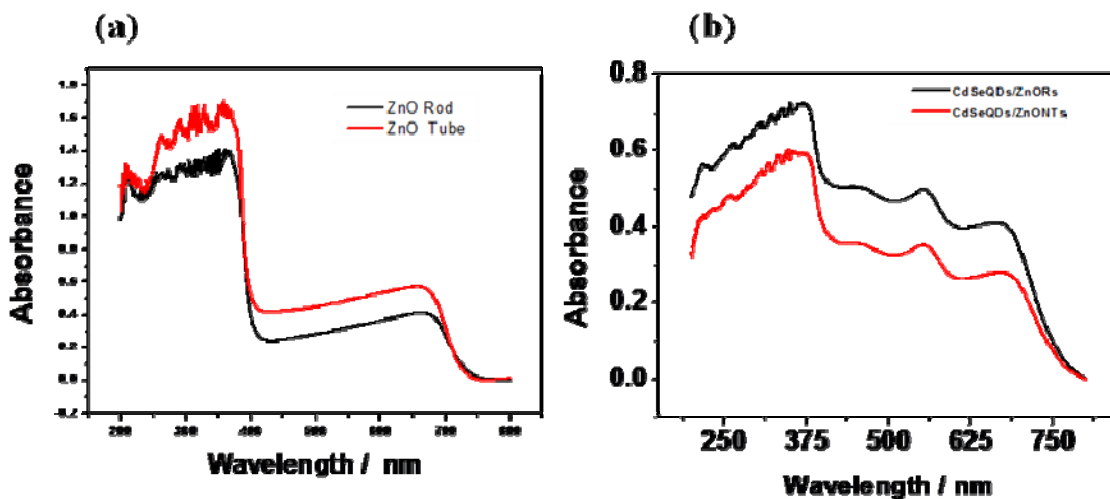


**Fig. S3** XRD patterns of (a) reference bulk ZnO (JCPDS:077-2205) and(b) reference CdSe (JCPDS:077-0021) (c) as synthesized ZnO NTs, (d) ZnO NTs@CdSe(QDs) and (e) annealed ZnO NTs@CdSe(QDs). Cross signs assigned to the substrate FTO peaks.

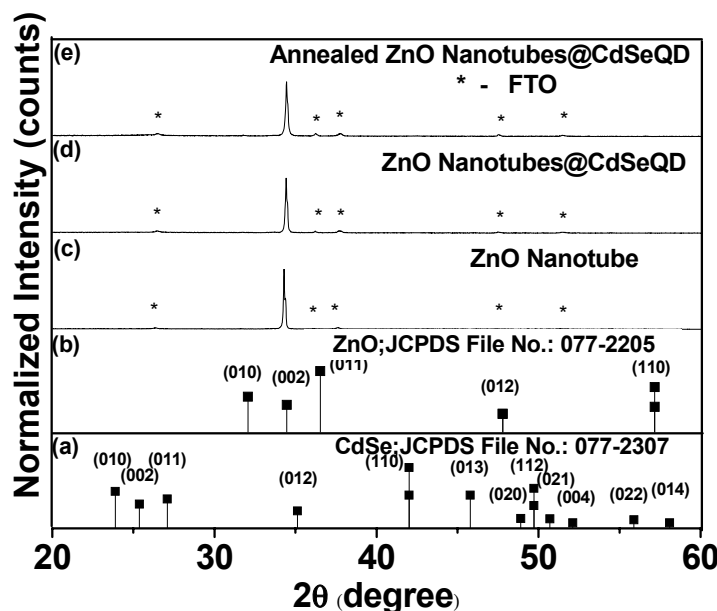


**Fig. S4** (Color on line) XRD patterns of pristine ZnO NTs (black line), ZnO NTs@CdSe(QDs) (red line) and annealed ZnO NTs@CdSe(QDs) (green line). Specific peak (110) ( $2\theta = 42.02$  JCPDS File No. 077-2307) of hexagonal CdSe observed upon careful examination of the pattern.

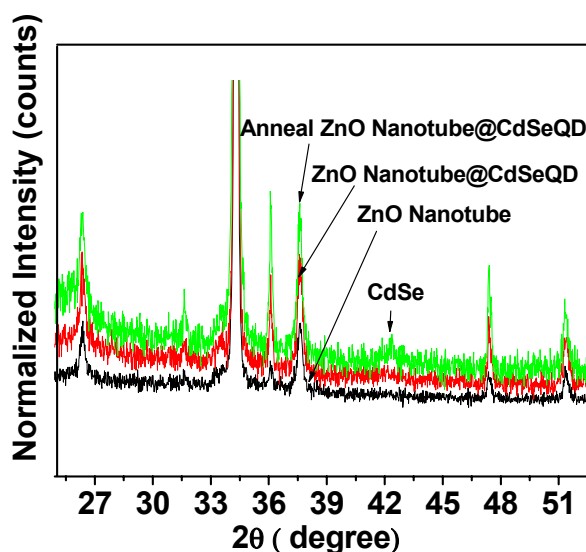


**Fig. S5** HRTEM nanographs of ZnO NTs@CdSe(QDs) samples (a) before annealing and (b) after annealing conditions.

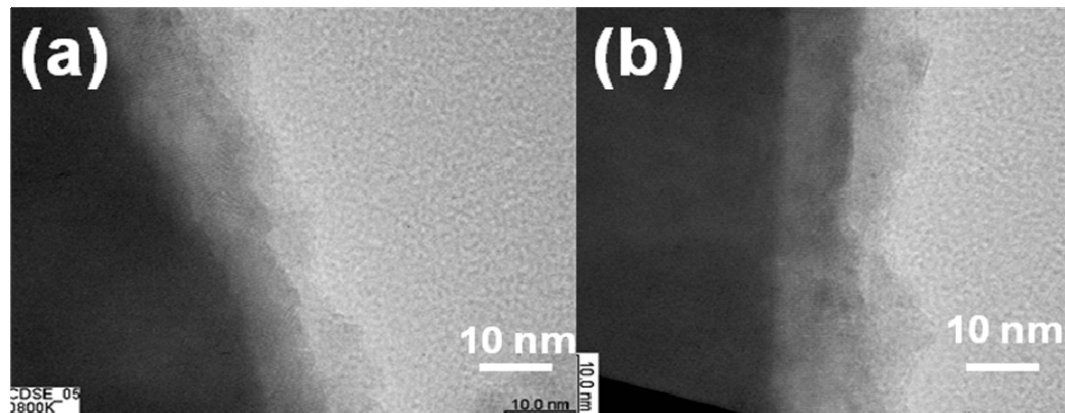


**Fig. S6** Photoluminescence emission spectrum of 3.06 nm TOPO escorted- CdSe QDs solutions excited by a 354 nm light source and micrographic TEM image of TOPO escorted- CdSe QDs has been showcased in inset.

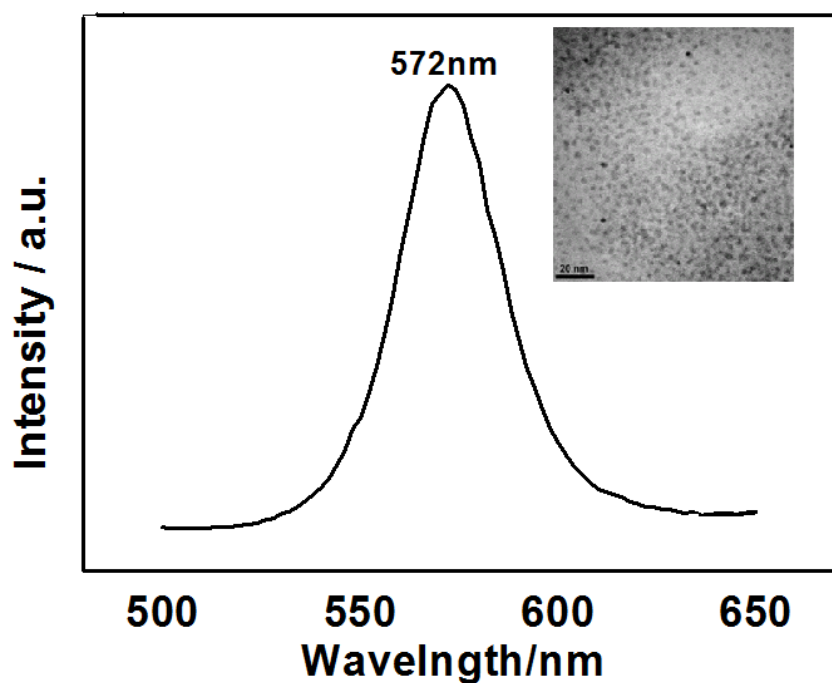


**Fig. S7** FE-SEM images of (a) top view of ZnO NRs (b) regular hexagonal shaped ZnO uncooled-nanorod samples.

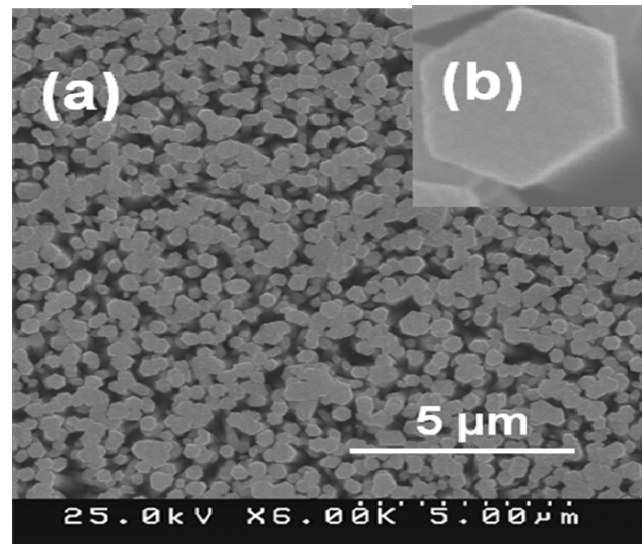


**Fig. S8** XANES (O K- edge) spectra of bulk ZnO (black-line), ZnO NRs (red dotted line) and ZnO NTs (green dotted line), indicating a red shift caused by the change in lattice parameters to maintain a constant Zn-O bond length.

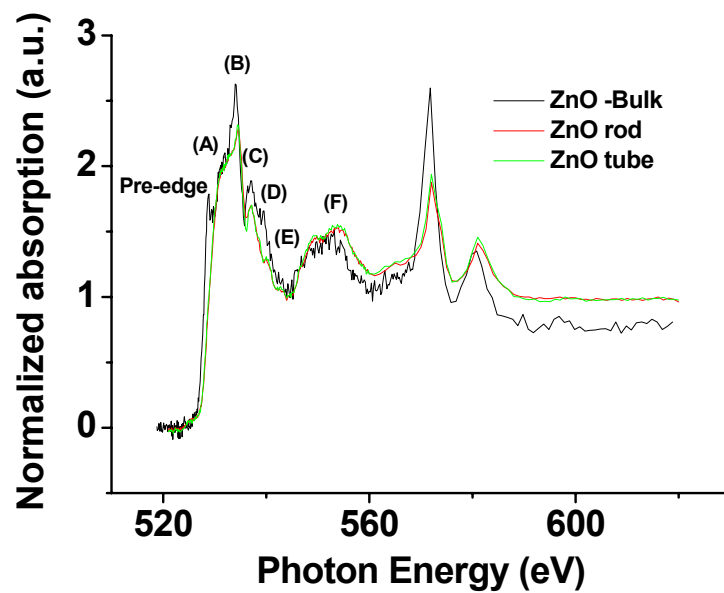


**Fig. S9** Linear sweep voltammogram for various loadings of CdSe QDs on arrays of ZnO NTs in aqueous 0.35 M Na<sub>2</sub>S and 0.25 M K<sub>2</sub>SO<sub>3</sub> electrolyte (pH =13.3) under illumination of power density 100 mW/cm<sup>2</sup>( AM1.5G).

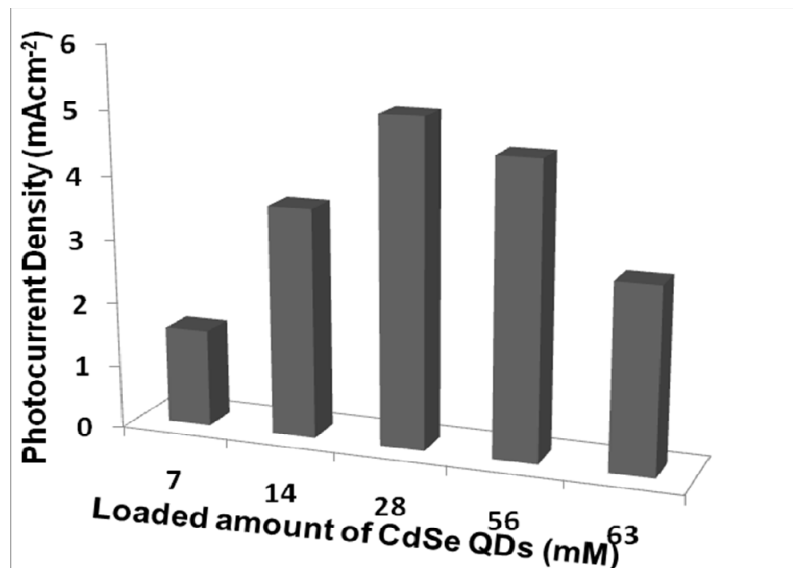


**Fig. S10** Cyclic voltammetric plots as a function of photocurrent density *Vs* applied potential (with respect to SCE) for ZnO NTs, ZnO NTs@CdSe(QDs) and annealed ZnO NTs@CdSe(QDs) in aqueous 0.35 M Na<sub>2</sub>S and 0.25 M K<sub>2</sub>SO<sub>3</sub> electrolyte (pH =13.3) under illumination of 100 mW/cm<sup>2</sup>( AM1.5G) power density and ~1 cm<sup>2</sup> exposure area of working electrode.

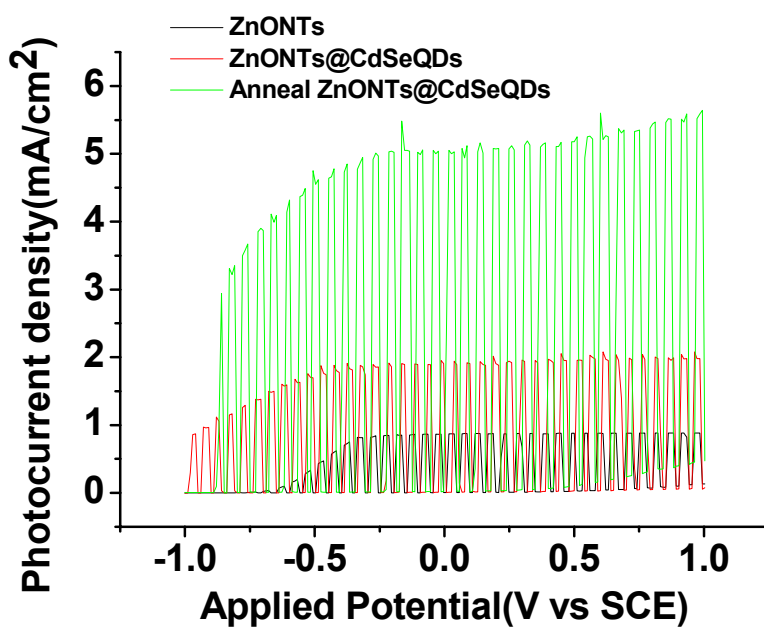


**Fig. S11** Snap shot of annealed ZnO NTs@CdSe(QDs), ZnO NTs@CdSe(QDs) and ZnO NTs (a) taken in ordinary light and (b) taken in UV light, respectively.



**Fig. S12.** Representative spectral distribution of Xe light source with the filter PE300BF in visible light region (390-770 nm). Where F denotes UV output, UV represented the ultra violet filtered output and F-HOT- MIRROR exhibited UV filter output reflected through hot mirror.

